Time-Dependent Mechanochemical Response of SP-Cross-Linked PMMA

Cassandra M. Degen,*[†,∥,⊥] Preston A. May,[‡,∥] Jeffrey S. Moore,[‡,∥] Scott R. White,[§,∥] and Nancy R. Sottos[†,∥]

[†]Department of Materials Science and Engineering, University of Illinois at Urbana−Champaign, 1304 W. Green Street, Urbana, Illinois 61801, United States

[‡]Department of Chemistry, University of Illinois at Urbana−Champaign, 505 S. Mathews Avenue, Urbana, Illinois 61801, United States

[§]Department of Aerospace Engineering, University of Illinois at Urbana−Champaign, 104 S. Wright Street, Urbana, Illinois 61801, United States

[∥]Beckman Institute for Advanced Science and Technology, University of Illinois at Urbana−Champaign, 405 N. Mathews Avenue, Urbana, Illinois 61801, United States

S Supporting Information

ABSTRACT: Time-dependent mechanochemical activation of spiropyran (SP) mechanophores in cross-linked PMMA under creep loading is examined. In contrast to monotonic torsion (constant strain rate) results, the desired force-induced electrocyclic ring-opening of SP to the fluorescent merocyanine (MC) form is achieved at creep stress levels less than the yield stress of the bulk polymer. Lower values of stress require longer time, but much smaller strains for initiation of activation. Additionally, the first measurable detection of the reaction corresponds closely to the maximum creep strain rate, revealing mechanophore activation occurs near the onset of strain hardening, when polymer mobility is highest. The strong correlation between mechanical activation of the spiropyran and the rate of deformation suggests the potential for SP mechanophores as molecular probes of polymer relaxation and flow.
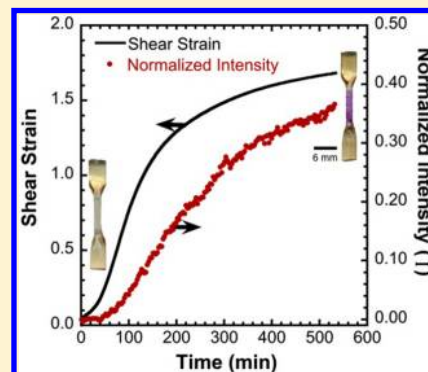
INTRODUCTION

Force-induced chemical changes in polymers enable a range of interesting properties including changes in color, fluorescence, conductivity, and stiffness.[1,2] Mechanoresponsive polymers are achieved through several different strategies,[3−6] and recently, Hickenboth et al.[7] introduced a powerful synthetic approach to create mechanoresponsive polymers in which force-activated mechanophores are linked directly into polymer chains. The mechanophore motif requires efficient transfer of external force to a relatively small number of specific bonds in the bulk polymer.[8−10] A diverse range of mechanophores have been investigated, each with a unique chemical signature upon activation.[7,11−23]

The mechanophore investigated in this paper, spiropyran (SP), provides evidence of a local chemical reaction (an electrocyclic ring-opening) by reversibly transforming from a closed, colorless SP form into a highly colored and fluorescent merocyanine (MC) molecule by rupture of the spiro carbon−oxygen (C−O) bond (Figure 1). SP is known to transform to the MC form with UV light as well as heat and is reversible with visible light. As first shown by Potisek et al.,[22] mechanical force provides an additional pathway for the ring-opening to occur as indicated by a visible color change of a solution of SP-linked PMA in solution after sonication. Davis et al.[24] successfully

showed selective activation, and consequent visible color change, of the SP mechanophore linked in linear PMA during tension and in cross-linked poly(methyl methacrylate) (PMMA) during diametric compression. Davis[24] observed strain rate sensitivity and the need for large plastic strain to achieve activation but lacked quantitative *in situ* analysis of the SP to MC transformation.

Additional studies of the SP mechanophore in bulk polymers reveal that the transfer of macroscopic force to the SP molecule, and subsequent activation to the merocyanine (MC) form, is inherently tied to the mechanical behavior of the polymer[25−28] and polymer architecture, mobility, chain orientation, and external loading conditions. Examining a chain-centered mechanophore in PMMA, Beiermann et al.[25] determined a critical temperature window over which SP activated, coinciding with conditions necessary to achieve polymer yielding and drawing. Polymer chain orientation was also an important factor contributing to SP activation,[26] suggesting that the reaction can be tuned by altering the polymeric structure. As a cross-linker in PMMA, SP was found to activate after large-
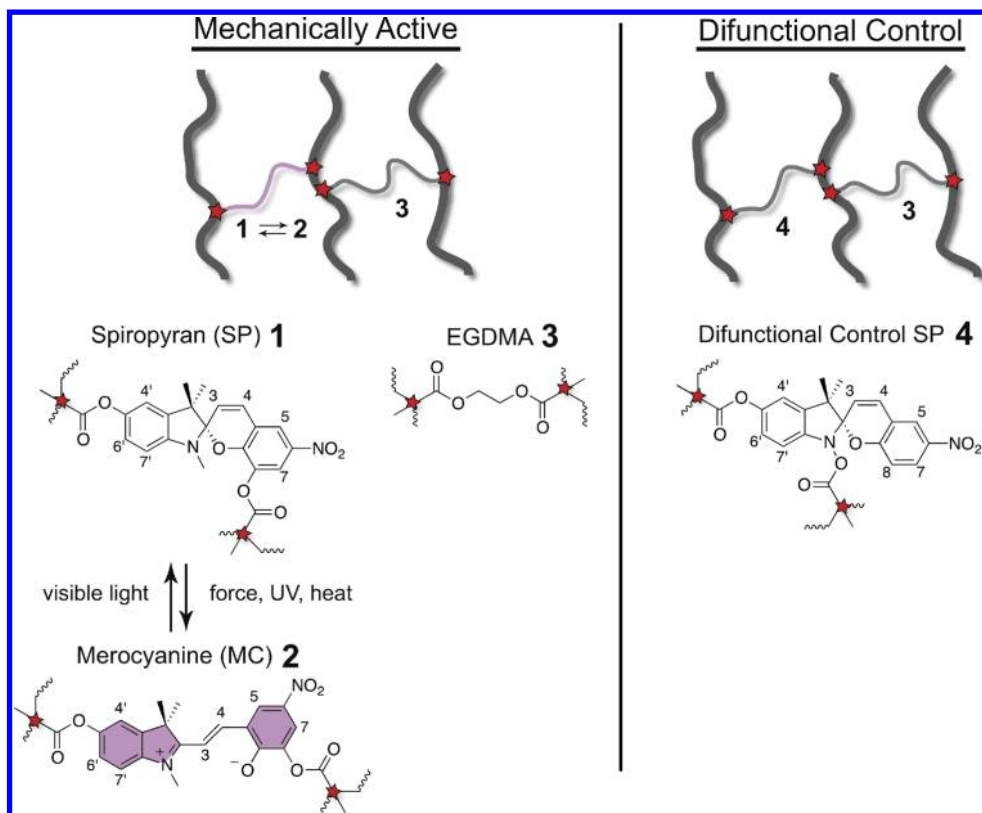
Figure 1. Architecture of active and control cross-linked PMMA polymers.
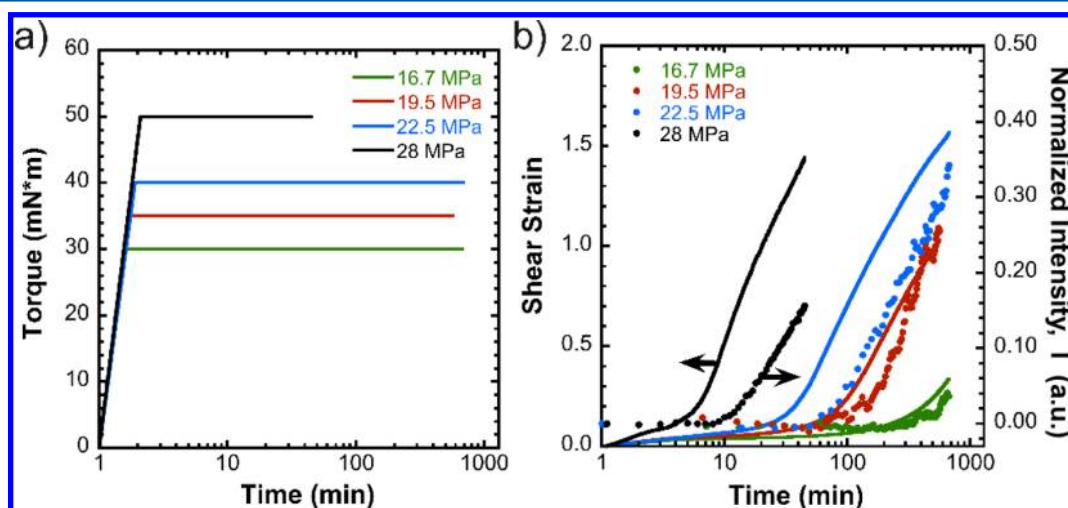

Figure 2. Rheometer torque profiles and corresponding creep strain and fluorescence data. (a) Representative input torque profiles and corresponding creep stress levels. (b) Representative evolution of shear strain (solid line) and normalized intensity (dotted curve) as a function of time for various creep stress levels.

scale polymer deformation and flow and is influenced by factors that affect polymer yield such as polymer architecture and strain rate.[24,29] After incorporating SP in polycaprolactone, O'Bryan et al.[27] measured the force induced by the MC to SP transformation when driven by white light under constant strain. Lee et al.[28] incorporated SP in polyurethane and demonstrated that the SP–MC equilibrium was shifted to the MC form when the polymers were held at constant strain. Lee et al.[28] also investigated the time constant of the reversion of MC to SP through fluorescence decay, concluding that the reversion is influenced by relaxation of residual strain after deformation.

Using the full field fluorescence technique reported previously by Kingsbury et al.,[29] we simultaneously track the evolution of fluorescence and creep strain in SP-cross-linked PMMA at different stress levels. Fluorescent probes have been previously incorporated as additives and utilized to investigate molecular processes during deformation.[30−33] Similarly, the observed correlation of mechanophore activation with changes in creep strain in this paper reveals the potential for the SP cross-linker to act as a molecular probe of polymer relaxation and creep mechanisms.
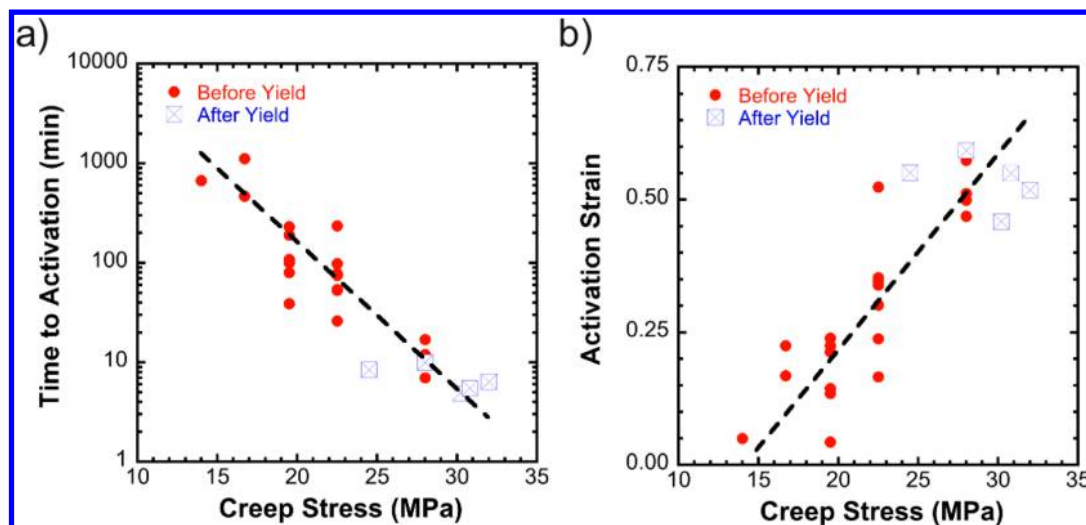
Figure 3. Activation characterization of PMMA-SP under creep. (a) Time to activation and (b) activation strain (as defined when $\overline{I} = 0.01$) as a function of creep stress level. Data have been color-coded to indicate applied torque profiles both before (red) and after yield (blue).

EXPERIMENTAL SECTION

Materials. Poly(methyl methacrylate) (PMMA) cross-linked with co-cross-linkers of ethylene glycol dimethacrylate (EGDMA) (**3**) and spiropyran (SP) (**1**) was synthesized by free-radical polymerization initiated with benzoyl peroxide and dimethylaniline at room temperature. Polymerizations were performed according to Kingsbury et al.,[29] and the total cross-link density was kept constant at 1 mol % (0.018 mol % SP, 0.982 mol % EGDMA). The architecture of the cross-linked PMMA is shown in Figure 1.

Torsion samples were polymerized in preshaped syringe molds for 24 h immersed in a room temperature water bath to reduce the effect of exothermic heating during polymerization. The resulting cylindrical samples had a gauge section of 10 mm in length and 2 mm in diameter.

Control samples were synthesized with difunctional SP (**4**), as shown in Figure 1. The polymer attachment points at the 5′ and 8 positions in the difunctional SP molecule precluded force transfer across the reactive C−O spiro-bond. Although the mechanical pathway was eliminated, conversion of SP to MC after exposure to UV light or heat was confirmed by visible color change in all control specimens.

Torsional Creep. Torsional creep experiments were conducted at room temperature (~19 °C) with a TA Instruments AR-G2 rheometer and custom torsion grips. Samples were subject to a constant strain rate of 10^{-3} s^{-1} until a desired torque level was achieved. Torque was held constant, and the rotational response was monitored as a function of time. Representative torque profiles are shown in Figure 2a. Torque levels studied corresponded to shear stress levels achieved both before and after the monotonic polymer yield as described in the Supporting Information (Figure SI.1).

Shear strain (γ) was calculated from rotation data accounting for large deformation following Wu et al.[34]

$$\gamma = r\left(1 - \frac{1}{2}A(\theta)\right)\theta \tag{1}$$

where r is the initial sample radius, θ is the rotation in radians, and $A(\theta)$ is the axial strain induced in the gauge section during torsion. The creep stress, τ, on the torsion sample subject to an applied torque (M) hold step is given by[34]

$$\tau = \frac{1}{2\pi r^3}\left(3M + \theta\frac{dM}{d\theta}\right)\left(\frac{1}{1 - \frac{1}{2}\left(3A(\theta) + \theta\frac{dA(\theta)}{d\theta}\right)}\right) \tag{2}$$

Full Field Fluorescence Imaging. Prior to testing, all samples were exposed to intense white light for 24 h to drive the

mechanophores to the photostationary closed SP state. During torsional creep, full field fluorescence (FFF) images were collected following the method described by Kingsbury et al.[29] The torsion sample was illuminated by 400−550 nm light, and a Basler CCD camera was positioned at 90° to the illumination source to collect 600−1200 nm light. To minimize photobleaching of the MC during the long testing times of torsional creep experiments, a mechanical shutter was placed in front of the illumination source and opened at discrete time intervals to permit imaging. LabView software was used to simultaneously control the shutter and collect images on a computer.

Fluorescence Data Analysis. Fluorescence data were analyzed using the method described by Kingsbury et al.[29] A normalized intensity ($\overline{I}$) was calculated according to

$$\overline{I} = \frac{I(\gamma) - I(\gamma = 0)}{I_{max} - I_{min}} \tag{3}$$

where $I(\gamma)$ is the intensity of a particular sample at a given shear strain, $I(\gamma = 0)$ is the intensity of the sample at zero shear strain, and I_{max} and I_{min} are the maximum (photostationary MC form) and minimum (photostationary SP form) intensities of a UV polymerized, and subsequently photobleached, sample. The normalized intensity ($\overline{I}$) was fit to a cumulative Weibull curve, and the onset of activation was defined when the normalized intensity increased by 1% from the initial value ($\overline{I} = 0.01$). This value was used to determine the corresponding activation strain and time to activation for each creep stress level.

RESULTS AND DISCUSSION

Simultaneous measurements of creep strain and normalized fluorescence intensity were collected at different stress levels. Representative data are plotted as a function of time in Figure 2b. Below a creep stress of approximately 16 MPa very little shear strain accumulated, and no detectable fluorescence was observed. These samples also showed no visual color change, in contrast to those tested at higher creep stress levels. Control samples containing either difunctional SP (**4**) or no SP showed minimal changes in fluorescence intensity (Figure SI.2) and no visible color change.

Analysis of the onset of activation based on fluorescence intensity reveals a decrease in the time to activation (Figure 3a) and an increase in the corresponding activation strain value (Figure 3b) with increasing creep stress magnitude. During torsional creep at lower applied stress levels, the creep rate is slow and the polymer accumulates minimal shear strain during

the long time period required for mechanochemical activation. At higher stress levels, the creep rate is much faster, and during the short time interval required for activation, the polymer is able to undergo larger deformation.

Mechanochemical activation was further examined as a function of creep rate ($d\gamma/dt$). Figure 4 shows the evolution of
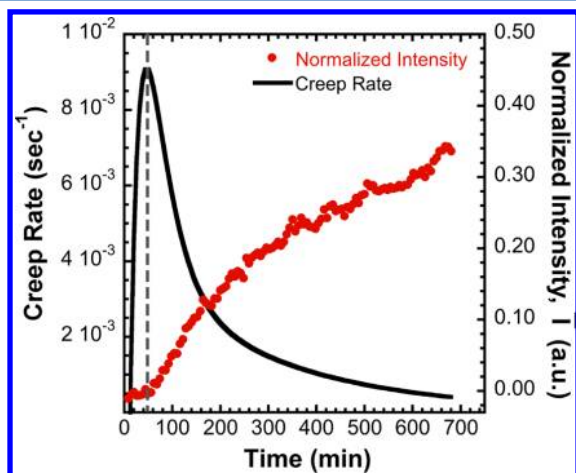

Figure 4. Representative creep rate and normalized intensity as a function of time at a creep stress of 22.5 MPa. Activation occurs at the maximum creep rate as indicated by the dashed line.

fluorescence intensity and creep rate for a stress level of 22.5 MPa. The vertical dashed line in Figure 4 indicates the activation point ($\overline{I} = 0.01$). The onset of activation determined from the optical FFF method coincides with the maximum creep rate determined solely from the rheometric torque–rotation data. Figure 5 more clearly reveals the one-to-one relationship between the time to activation and the time at which the maximum creep rate occurs for all creep stress levels studied. The peak in the creep rate is associated with the onset of strain hardening.[35] Moreover, the physical mechanisms
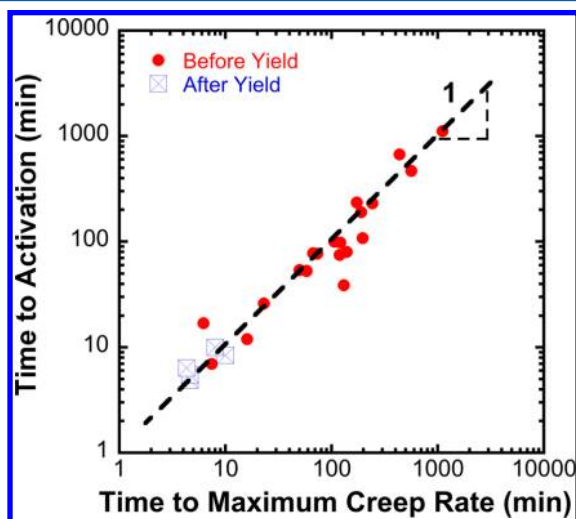

Figure 5. Correlation of the time to activation as determined optically from full field fluorescence imaging to the time of maximum creep rate as determined from rheometric torque–rotation data. A slope of 1 shown by the dashed line indicates mechanophore activation occurs as the polymer reaches the maximum creep rate. Data have been color-coded to indicate applied torque profiles both before (red) and after (blue) yield.

associated with strain hardening in polymer glasses are closely related to plastic flow.[36] Hence, mechanochemical activation in a mechanophore-cross-linked polymer is correlated with macroscopic strain hardening and plastic flow. This result is consistent with monotonic torsion investigations from Kingsbury et al.,[29] which showed the polymer must be loaded beyond the yield stress and plastic deformation must be induced to initiate activation.

The relationship between mechanochemical activation of SP from previous monotonic torsion results[29] and torsional creep in this work is shown in Figure 6. For both loading cases, the
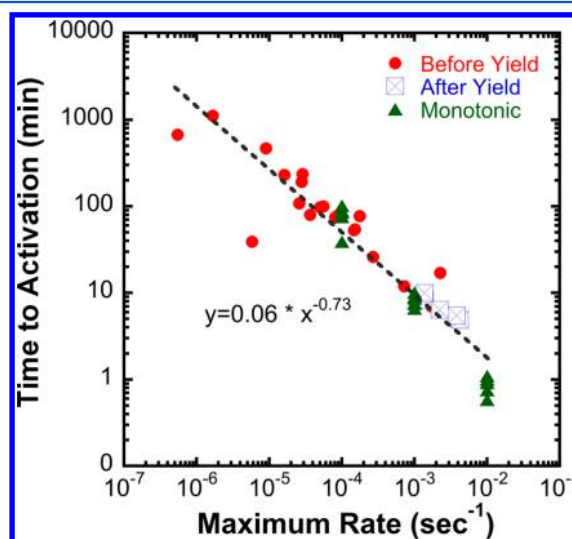

Figure 6. Time to activation as a function of the maximum strain rate during torsion testing. Torsional creep data and monotonic torsion data[29] follow the same trend line. Creep data have been color-coded to indicate applied torque profiles both before (red) and after (blue) yield and is shown with monotonic torsion data (green).

time required for activation decreases as the maximum strain rate increases. In response to high strain rates, the forces imparted to the mechanophore through polymer chains are higher, allowing mechanophore activation to occur quickly. In contrast, at low strain rates the force applied to the SP molecule is lower, and longer times are required to initiate activation. Similar to prior experimental,[30−33,37] numerical,[38] and theoretical[39] results which report a strong correlation between molecular mobility and strain rate, the activation of SP in cross-linked PMMA requires stress-induced mobility, as implied in Figure 6.

Figure 6 reveals a power law relationship between the time required for activation and the rate of deformation of the mechanochemically active polymer

$$t = A(\dot{\gamma})^n \tag{4}$$

where t is the time to activation of SP, $\dot{\gamma}$ is the shear strain rate, and A and n are fitting parameters. A best fit of the data collected for both monotonic torsion and torsional creep gives the unitless fitting parameters of A and n as 0.06 and −0.73, respectively. This relationship may help predict mechanochemical response at strain rates beyond the scope of this work. At very fast rates of deformation, activation of SP will eventually compete with the time scale of fracture of the bulk polymer. Fracture testing of mechanochemically active polymers coupled with FFF or other detection schemes could provide

complementary results to these studies of monotonic torsion and torsional creep.

CONCLUSION

A full field fluorescence method was adapted to successfully characterize the mechanochemical activation of SP in cross-linked PMMA during torsional creep deformation. In contrast to previous monotonic studies,[29] mechanical activation of SP was achieved at stress levels below the monotonic polymer yield stress. As the creep stress level was increased, the time required for the onset of activation decreased, but the corresponding strain value at activation increased. Additionally, the onset of the activation correlated to a maximum in the creep strain rate for each stress level tested, suggesting that mechanochemical activity is favored when strain hardening is initiated in the polymer. These data further confirm the need for large-scale polymer deformation, the onset of flow, and stress-induced mobility to achieve mechanochemical activation of SP. Moreover, the SP mechanophore also has the potential to serve as a molecular probe of polymer deformation mechanisms, and the role of force transfer from polymer chains to mechanophores can be used to guide the design of mechanoresponsive materials with targeted engineering applications.

ASSOCIATED CONTENT

Ⓢ Supporting Information

Details of torsional creep procedure, representative shear strain and normalized intensity data of control samples, and details on the synthesis of difunctional SP (**4**). This material is available free of charge via the Internet at http://pubs.acs.org.

AUTHOR INFORMATION

Corresponding Author
*E-mail: Cassandra.Degen@sdsmt.edu (C.M.D.).

Present Address
[⊥]C.M.D.: Department of Mechanical Engineering, South Dakota School of Mines and Technology, 501 E. St. Joseph Street, Rapid City, SD 57701.

Notes
The authors declare no competing financial interest.

ACKNOWLEDGMENTS

REFERENCES

(1) Beyer, M. K.; Clausen-Schaumann, H. *Chem. Rev.* **2005**, *105*, 2921.
(2) Caruso, M. M.; Davis, D. A.; Shen, Q.; Odom, S. A.; Sottos, N. R.; White, S. R.; Moore, J. S. *Chem. Rev.* **2009**, *109*, 5755.
(3) Lowe, C.; Weder, C. *Adv. Mater.* **2002**, *14*, 1625.
(4) Kim, S.-J.; Reneker, D. H. *Polym. Bull.* **1993**, *31*, 367.
(5) Nallicheri, R. A.; Rubner, M. F. *Macromolecules* **1991**, *24*, 517.
(6) Foulger, S. H.; Jiang, P.; Lattam, A. C.; Smith, D. W. J.; Ballato, J. *Langmuir* **2001**, *17*, 6023.
(7) Hickenboth, C. R.; Moore, J. S.; White, S. R.; Sottos, N. R.; Baudry, J.; Wilson, S. R. *Nature* **2007**, *446*, 423.
(8) Kausch, H. H. *Colloid Polym. Sci.* **1985**, *263*, 306.
(9) Kausch, H. H.; Plummer, C. J. G. *Polymer* **1994**, *35*, 3848.
(10) Dopieralski, P.; Anjukandi, P.; Rückert, M.; Shiga, M.; Ribas-Arino, J.; Marx, D. *J. Mater. Chem.* **2011**, *21*, 8309.
(11) Wiggins, K. M.; Hudnall, T. W.; Shen, Q.; Kryger, M. J.; Moore, J. S.; Bielawski, C. W. *J. Am. Chem. Soc.* **2010**, *132*, 3256.
(12) Kryger, M. J.; Munaretto, A. M.; Moore, J. S. *J. Am. Chem. Soc.* **2011**, *133*, 18992.
(13) Wiggins, K. M.; Syrett, J. A.; Haddleton, D. M.; Bielawski, C. W. *J. Am. Chem. Soc.* **2011**, *133*, 7180.
(14) Klukovich, H. M.; Kean, Z. S.; Ramirez, A. L. B.; Lenhardt, J. M.; Lin, J.; Hu, X.; Craig, S. L. *J. Am. Chem. Soc.* **2012**, *134*, 9577.
(15) Berkowski, K. L.; Potisek, S. L.; Hickenboth, C. R.; Moore, J. S. *Macromolecules* **2005**, *38*, 8975.
(16) Paulusse, J. M. J.; Sijbesma, R. P. *Angew. Chem., Int. Ed.* **2004**, *43*, 4460.
(17) Karthikeyan, S.; Potisek, S. L.; Piermattei, A.; Sijbesma, R. P. *J. Am. Chem. Soc.* **2008**, *130*, 14968.
(18) Kryger, M. J.; Ong, M. T.; Odom, S. A.; Sottos, N. R.; White, S. R.; Martinez, T. J.; Moore, J. S. *J. Am. Chem. Soc.* **2010**, *132*, 4558.
(19) Tennyson, A. G.; Wiggins, K. M.; Bielawski, C. W. *J. Am. Chem. Soc.* **2010**, *132*, 16631.
(20) Brantley, J. N.; Wiggins, K. M.; Bielawski, C. W. *Science* **2011**, *333*, 1606.
(21) Lenhardt, J. M.; Black, A. L.; Craig, S. L. *J. Am. Chem. Soc.* **2009**, *131*, 10818.
(22) Potisek, S. L.; Davis, D. A.; Sottos, N. R.; White, S. R.; Moore, J. S. *J. Am. Chem. Soc.* **2007**, *129*, 13808.
(23) Brantley, J. N.; Wiggins, K. M.; Bielawski, C. W. *Polym. Int.* **2012**, *62*, 2.
(24) Davis, D. A.; Hamilton, A.; Yang, J.; Cremar, L. D.; Van Gough, D.; Potisek, S. L.; Ong, M. T.; Braun, P. V.; Martinez, T. J.; White, S. R.; Moore, J. S.; Sottos, N. R. *Nature* **2009**, *459*, 68.
(25) Beiermann, B. A.; Davis, D. A.; Kramer, S. L. B.; Moore, J. S.; Sottos, N. R.; White, S. R. *J. Mater. Chem.* **2011**, *21*, 8443.
(26) Beiermann, B. A.; Kramer, S. L. B.; Moore, J. S.; White, S. R.; Sottos, N. R. *ACS Macro Lett.* **2012**, *1*, 163.
(27) O'Bryan, G.; Wong, B. M.; McElhanon, J. R. *ACS Appl. Mater. Interfaces* **2010**, *2*, 1594.
(28) Lee, C. K.; Davis, D. A.; White, S. R.; Moore, J. S.; Sottos, N. R.; Braun, P. V. *J. Am. Chem. Soc.* **2010**, *132*, 16107.
(29) Kingsbury, C. M.; May, P. A.; Davis, D. A.; White, S. R.; Moore, J. S.; Sottos, N. R. *J. Mater. Chem.* **2011**, *21*, 8381.
(30) Krongauz, V. A.; Bosnjak, C. P.; Chudnovsky, A. *High Energy Chem.* **2009**, *43*, 400.
(31) Lee, H. N.; Paeng, K.; Swallen, S. F.; Ediger, M. D. *J. Chem. Phys.* **2008**, *128*, 134902.
(32) Lee, H. N.; Paeng, K.; Swallen, S. F.; Ediger, M. D. *Science* **2009**, *323*, 231.
(33) Tran-Cong, Q.; Chikaki, S.; Kanato, H. *Polymer* **1994**, *35*, 4465.
(34) Wu, H. C.; Xu, Z. Y.; Wang, P. T. *J. Test Eval.* **1992**, *20*, 396.
(35) Falk, M. L.; Langer, J. S. *Phys. Rev. E* **1998**, *57*, 7192.
(36) Haward, R. N. *The Physics of Glassy Polymers*, 2nd ed.; Chapman & Hall: London, 1997.
(37) Martinez-Vega, J. J.; Trumel, H.; Gacougnolle, J. L. *Polymer* **2002**, *43*, 4979.
(38) Riggleman, R. A.; Schweizer, K. S.; de Pablo, J. J. *Macromolecules* **2008**, *41*, 4969.
(39) Eyring, H. *J. Chem. Phys.* **1936**, *4*, 1901.
(40) Gottlieb, H. E.; Kotlyar, V.; Nudelman, A. *J. Org. Chem.* **1997**, *62*, 7512.